Hardness and Second Phase Percentage of Ni-Ti-Hf Compounds After Heat Treatment at 700 °C

Malcolm K. Stanford
Glenn Research Center, Cleveland, Ohio

NASA STI Program . . . in Profile

Since its founding, NASA has been dedicated to the advancement of aeronautics and space science. The NASA Scientific and Technical Information (STI) Program plays a key part in helping NASA maintain this important role.

The NASA STI Program operates under the auspices of the Agency Chief Information Officer. It collects, organizes, provides for archiving, and disseminates NASA's STI. The NASA STI Program provides access to the NASA Technical Report Server—Registered (NTRS Reg) and NASA Technical Report Server—Public (NTRS) thus providing one of the largest collections of aeronautical and space science STI in the world. Results are published in both non-NASA channels and by NASA in the NASA STI Report Series, which includes the following report types:

- TECHNICAL PUBLICATION. Reports of completed research or a major significant phase of research that present the results of NASA programs and include extensive data or theoretical analysis. Includes compilations of significant scientific and technical data and information deemed to be of continuing reference value. NASA counter-part of peer-reviewed formal professional papers, but has less stringent limitations on manuscript length and extent of graphic presentations.

- TECHNICAL MEMORANDUM. Scientific and technical findings that are preliminary or of specialized interest, e.g., "quick-release" reports, working papers, and bibliographies that contain minimal annotation. Does not contain extensive analysis.

- CONTRACTOR REPORT. Scientific and technical findings by NASA-sponsored contractors and grantees.

- CONFERENCE PUBLICATION. Collected papers from scientific and technical conferences, symposia, seminars, or other meetings sponsored or co-sponsored by NASA.

- SPECIAL PUBLICATION. Scientific, technical, or historical information from NASA programs, projects, and missions, often concerned with subjects having substantial public interest.

- TECHNICAL TRANSLATION. English-language translations of foreign scientific and technical material pertinent to NASA's mission.

For more information about the NASA STI program, see the following:

- Access the NASA STI program home page at http://www.sti.nasa.gov

- E-mail your question to help@sti.nasa.gov

- Fax your question to the NASA STI Information Desk at 757-864-6500

- Telephone the NASA STI Information Desk at 757-864-9658

- Write to:
  NASA STI Program
  Mail Stop 148
  NASA Langley Research Center
  Hampton, VA 23681-2199

Hardness and Second Phase Percentage of Ni-Ti-Hf Compounds After Heat Treatment at 700 °C

Malcolm K. Stanford
Glenn Research Center, Cleveland, Ohio

Acknowledgments

Hardness and Second Phase Percentage of Ni-Ti-Hf Compounds After Heat Treatment at 700 °C

Malcolm K. Stanford
National Aeronautics and Space Administration
Glenn Research Center
Cleveland, Ohio 44135

Abstract

The Vickers hardness and second phase precipitation of three ternary intermetallic Ni-Ti-Hf compounds containing either 1, 3 or 5 at.% Hf were compared to 60-Nitinol (55 at.% Ni – 45 at.% Ti). Heat treatment either at 700 °C or with a subsequent aging step, hardened the 3 and 5 at.% Hf-containing ternaries to approximately 620 HV (56 HRC). Heat treatment increased the hardness of the 1 at.% Hf compound by more than 25 percent. Average hardness of the 3 and 5 at.% Hf ternaries, though higher than that of the binary Ni-Ti or the Ni-Ti-Hf compound containing 1 at.% Hf, appeared to be fairly insensitive to the different heat treatments. There was a drastic reduction of fatigue-enhancing second phase precipitates for the 5 at.% Hf ternaries compared to the other compounds. These results should guide materials selection for development of aerospace componentry.

Introduction

The alloy 60-Nitinol (60 wt.% Ni – 40 wt.% Ti or 55 at.% Ni – 45 at.% Ti) is a superelastic material that has been under development by NASA for aerospace ball bearing applications (Refs. 1 to 3). The material can be hardened for use in this application with a relatively simple heat treatment: 900 °C for 2 hr followed by water quenching. This heat treatment renders the material with Vickers hardness of approximately 620 HV (equivalent to Rockwell C hardness of 56 HRC), which is acceptable for bearing applications. Heat treatment at higher temperatures (e.g., 1,000 °C for 2 hr followed by water quenching) yields a higher hardness (720 HV or 61 HRC), but heat treatment at these temperatures has been found to result in frequent quench cracking (Ref. 4). Therefore, an effort has been underway to address the issue of quench cracking in 60-Nitinol. One approach to this problem has been to introduce ternary elements to the Ni-Ti compound that make solution treatment at lower temperatures more thermodynamically favorable (Ref. 5). This paper reports results for one such ternary compound, namely Ni-Ti-Hf.

Thermally-induced stress σ_{therm} generated from cooling a material from T_2 to T_1 is linearly proportional to the elastic modulus E, the thermal expansion coefficient α, and the difference in temperatures according to Equation (1).

$$\sigma_{therm} = E\alpha(T_2 - T_1) \tag{1}$$

Quenching from 900 °C to room temperature would generate thermally-induced stresses of 8.9 MPa, based on physical properties reported elsewhere (Refs. 3 and 6). Depending on part geometry, these stresses could be compressive, tensile or shear in order to maintain static equilibrium. It is when residual stresses reach the failure strength of the material that quench cracking is possible. Previous studies estimate the tensile strength of 60-Nitinol at approximately 1,00 MPa (Refs. 3 and 7). Although this failure strength is more than one hundred times the thermally-induced strength, given the inherent brittleness of this material and the ability of flaws to initiate brittle fracture, the probability of quench cracking increases linearly with increasing heat treatment temperature, following Equation (1). There is a need, therefore, to reduce the heat treatment temperature necessary to harden this material for bearing applications.

This material hardens by the precipitation of a fine metastable Ni_4Ti_3 phase. The rapid quench is designed to prevent the subsequent formation of incoherent Ni_3Ti_2 or Ni_3Ti phases (Refs. 8 and 9). These phases not only soften the material by reducing the Ni available to form Ni_4Ti_3, but they create variations in the bulk modulus of the material, which could enhance crack formation during cyclic loading (Refs. 5, 10 to 12).

The purpose of this study was to characterize the hardness and microstructure of three Ni-Ti-Hf compounds after heat treatment at 700 °C, which is 200 °C lower than the heat treatment temperature currently used to heat treat 60-Nitinol (Ref. 13). Additionally, the effect of aging these compounds at 400 °C for 30 min (water quench) after the 700 °C heat treatment was studied. The results of this study should help guide process development for Ni-Ti-Hf components.

Procedures

Elemental Ni, Ti and Hf were purchased from commercial sources. The purity of each material was certified by the supplier with the chemical compositions listed in Table 1. These materials were used to fabricate small (50 g) ingots (55 at.% Ni with either 1, 3 or 5 at.% Hf, balance Ti) by vacuum arc remelting (Ref. 14). The compositions of the studied compounds and their designations for the present study are listed in Table 2. The ingots were homogenized for 48 hr at 1050 °C under vacuum (approximately 10^{-6} torr) followed by furnace cooling and then sectioned by wire electrical discharge machining into 5 mm cubic specimens. The chemical compositions of the studied compounds were analyzed by inductively-coupled plasma atomic emission spectroscopy (ICP-AES) (Ref. 15).

Two cubic specimens of each compound were heat treated for 2 hr at 700 °C in vacuum, followed by water quenching. One specimen of each compound was subsequently aged at 400 °C for 30 min and then water quenched. The specimens were prepared for metallographic examination, including optical and scanning electron microscopy. Vickers microindentation hardness was measured for the specimens after each heat treatment condition based on a standard procedure using a linear indentation spacing of 500 μm (Ref. 16). The average of 5 hardness measurements at each heat treatment condition was reported for each compound. No attempt was made to avoid grain boundaries during hardness testing. The percentage of secondary phases were measured using commercially-available software. This analysis took advantage of the difference in grey level from the parent phase (medium grey) to the precipitate phases (white), as described in detail elsewhere (Ref. 5). The composition of the phases in the microstructures were analyzed using scanning electron microscopy (SEM) and energy-dispersive x-ray spectroscopy (EDS) (Ref. 17).

Results

Hardness

The average microindentation hardness values for the studied compounds are shown in Figure 1. The hardness of Alloy 55 (55 at.% Ni – 45 at.% Ti), which is better known as *60-Nitinol* (60 wt.% Ni – 40 wt.% Ti), is included in the figure for comparison. The average hardness of the Hf-containing compounds is higher than that of Alloy 55 after homogenization or in either of the two heat treatment conditions. Also, the average hardness of the studied compounds tends to increase with increasing Hf content. The aging step appears to increase the average hardness for alloy 55-1H from 539 HV (after heat treatment at 700 °C) to 572 HV (after aging). Furthermore, the average hardness of alloy 55-1H after homogenization is approximately 454 HV, resulting in an increase in hardness of more than 25 percent after heat treating and aging.

For the 3 and 5 at.% Hf compounds, the average hardness varies from approximately 595 to 620 HV (about 55-56 HRC) after the 700 °C heat treatment and is nearly 620 HV after subsequent aging at 400 °C. This hardness is equivalent to that of 60 Nitinol after heat treatment at 900 °C for 2 hr followed

by water quenching (i.e., 56 HRC), the same heat treatment currently used to harden this alloy for component development studies at NASA (Ref. 13). Nevertheless, given the stated ranges of statistical variation, the average hardness of alloys 55-3H and 55-5H are effectively the same after either of the studied heat treatments and changes very little from the hardness of the compounds after homogenization. The effect aging may have on relieving residual stresses, while beyond the scope of this study, could be beneficial and will be a subject for future investigations.

Microstructure

The average percent volume of second phase is shown in Figure 2. Second phase volume varies between 26 and 38 percent for the compounds containing 0 to 3 at.% Hf, at either of the studied heat treatments. For the compound containing 5 at.% Hf, however, the average second phase volume drops to between approximately 2 and 6 percent for the two studied heat treatments. This reduction in second phase precipitates should improve fatigue behavior, as discussed previously. In fact, given the hardness of alloy 55-5H after homogenization and the low second phase volume, this compound should be considered for component development in the homogenized condition, where residual stresses would be very low. Although machinability could be more difficult due to the high hardness, near net-shape methods like powder injection molding could make the use of this compound highly feasible.

Optical micrographs of the studied compounds after homogenization and after the studied heat treatments are shown in Figures 3 to 5. These micrographs corroborate the quantitative data mentioned above, showing that alloys 55, 55-1H and 55-3H had much more observable second phase precipitation within the grains and along the grain boundaries than alloy 55-5H. The second phase precipitates also appear to become finer as the Hf content increased. The color of the second phase from alloys 55, 55-1H and 55-3H (which appear mostly white with a few small black precipitates) to alloy 55-5H (which appear only as small black precipitates) suggest a difference in the composition of the second phase. An analysis of the composition of the observed secondary phases is discussed below.

SEM micrographs of alloy 55 are shown in Figure 6. EDS analyses of the phases, shown in Figure 7 and quantified in Table 3, indicates that the blocky phase at the locations labeled A and B (Fig. 6(b)) is Ni_3Ti_2. The elongated phase at locations C and D (Figs. 6(b) and (c)) is identified as Ni_3Ti and the parent phase is identified as NiTi. The morphologies of these phases are similar to those reported previously by others (Refs. 8 and 9).

Figure 8 shows SEM micrographs of alloy 55-1H. For this alloy, EDS analyses (Fig. 9 and Table 4) reveals the presence of mostly Ni_3Ti_2 precipitates in a Ni(Ti,Hf) parent phase with a few sparse oxide and nitride phases. SEM micrographs of another area of alloy 55-1H are shown in Figure 10 with EDS analysis results given in Figure 11 and Table 4.

Analysis of alloy 55-5H, shown in Figure 12, indicates the presence of low levels of hafnium carbide and oxide phases within the Ni(Ti,Hf) parent phase (Fig. 13 and Table 5). These secondary phases are minor and probably result from the trace amounts of oxygen and carbon present in the precursor elemental materials (Table 1) but they are not expected to have a significant effect on the physical properties of this compound.

Summary

The hardness and second phase precipitation of intermetallic Ni-Ti-Hf alloys after heat treatment at 700 °C and after subsequent aging at 400 °C were studied. Based on this study, the following conclusions have been made:

1. Heat treatment at 700 °C can be used to harden the studied 3 and 5 at.% hafnium-containing compounds (alloys 55-3H and 55-5H) to approximately 620 HV (56 HRC), which is a hardness acceptable for bearing applications.

2. The hardness of alloys 55-3H and 55-5H is essentially the same after either the 700 °C heat treatment or the 700 °C heat treatment followed by aging at 400 °C.
3. The effect of heat treatment is much greater for alloy 55-1H than for alloys 55, 55-3H or 55-5H.
4. Compounds containing from 0 to 3 at.% Hf had between 26 and 38 percent second phase compared to alloy 55-5H, which showed only small levels of oxide or carbide inclusions within the Ni(Ti,Hf) parent phase.

References

1. C. DellaCorte, S.V. Pepper, R.D. Noebe, D.R. Hull and G. Glennon, Intermetallic Nickel-Titanium Alloys for Oil-Lubrication Bearing Applications, NASA/TM—2009-215646, March 2009.
2. S.V. Pepper, C. DellaCorte, R.D. Noebe, D.R. Hull and G. Glennon, Nitinol 60 as a Material for Spacecraft Trioelements, ESMATS 13 Conference, Vienna, Austria, September 2009.
3. C. DellaCorte, R.D. Noebe, M.K. Stanford, S.A. Padula, "Resilient and Corrosion-Proof Rolling Element Bearings Made From Superelastic Ni-Ti Alloys for Aerospace Mechanism Applications," NASA/TM—2011-217105, NASA Center for Aerospace Information, Hanover, MD, 2011.
4. M.K. Stanford, F. Thomas and C. DellaCorte, "Processing Issues for Preliminary Melts of the Intermetallic Compound 60-NITINOL," NASA/TM—2012-216044, National Aeronautics and Space Administration, Langley, VA, 2012.
5. M.K. Stanford, "Hardness and Microstructure of Binary and Ternary Nitinol Compounds," NASA/TM—2016-218946, National Aeronautics and Space Administration, Langley, VA, 2016.
6. M.K. Stanford, "Thermophysical Properties of 60-NITINOL for Mechanical Component Applications," NASA/TM—2012-216056, National Aeronautics and Space Administration, Langley, VA, 2012.
7. C. DellaCorte and W.A. Wozniak, "Design and Manufacturing Considerations for Shockproof and Corrosion-Immune Superelastic Nickel-Titanium Bearings for a Space Station Application," NASA/TM—2012-216015, National Aeronautics and Space Administration, Langley, VA, 2012.
8. R.R. Adharapurapu, F. Jiang and K.S. Vecchio, "Aging effects on hardness and dynamic compressive behavior of Ti-55Ni (at.%) alloy," Materials Science & Engineering A, vol. 527, pp. 1665–76, 2010.
9. M. Nishida, C.M. Wayman and T. Honma, "Precipitation Processes in Near-Equiatomic TiNi Shape Memory Alloys," Metallurgical Transactions A, Vol. 17A, 1986, pp. 1505–1515.
10. M.K. Stanford, "Charpy Impact Energy and Microindentation Hardness of 60-NITINOL, NASA/TM—2012-216029, National Aeronautics and Space Administration, Langley, VA, 2012.
11. B.C. Hornbuckle, R.D. Noebe and G.B. Thompson, Influence of Hf Solute Additions on the Precipitation and Hardenability in Ni-rich NiTi Alloys, Journal of Alloys and Compounds, Vol. 640, pp. 449–54, 2015.
12. B.C. Hornbuckle, Investigation in Phase Stability and Mechanical Attributes in Very Ni-rich Nitinol with and without Hafnium Additions, Ph.D. dissertation, University of Alabama, August 2014.
13. EM30 Technical Specification, "60Ni-40Ti Billets."
14. Choudhury, Vacuum Metallurgy, ASM International, Materials Park, OH, 1990.
15. L.M. Faires, "Inductively Coupled Plasma Atomic Emission Spectroscopy," in ASM Handbook, Vol. 10: Materials Characterization, pp. 31–42, ASM International, Materials Park, OH, 1986.
16. ASTM Designation E 384-11[ε1], "Standard Test Method for Knoop and Vickers Hardness of Materials," 2011, vol. 03.01, American Society for Testing and Materials, West Conshokocken, PA.
17. D.E. Leyden, "X-Ray Spectrometry," in ASM Handbook, Vol. 10, Materials Characterization, pp. 82–101, ASM International, Materials Park, OH, 1986.

TABLE 1.—COMPOSITION OF ELEMENTAL METALS USED AS PRECURSOR
MATERIALS IN THIS STUDY. ONLY THE IMPURITIES
GREATER THAN 1 ppm ARE INCLUDED

Element	Purity, percent	Major impurities, ppm
Ni	99.999	C (10), Fe (12), O (5), S (2)
Ti	99.995	C (11), Fe (5), H (1), N(<10), O (216), Rb (<5), S (<5), Sr (<3000), Ta (<5), Y (<200)
Hf	99.7	Al (<25), B (<0.5), C (<20), Cd (<3), Cr (<30), Co (<5), Cu (<20), Fe (<50), H (<3), Mg (<10), N (<5), Nb (<50), Ni (<25), O (<53), P (<3), Pb (<5), S (<10), Si (<25), Sn (<10), Th (<4), Ti (<20), U (<2), V (<10), W (<20), Zr (14000)

TABLE 2.—COMPOSITION OF THE COMPOUNDS STUDIED IN THIS INVESTIGATION

Designation	Measured composition, wt.% [at.%]			Impurities, ppm
	Ni	Ti	Hf	
Alloy 55	59.1 [54.2]	40.7 [45.8]	0 [0]	Al (10), Co (20), Cu (100), Fe (10), Mo (30), W (1300), C (80), N (<10), O (220)
Alloy 55-1H	56.9 [53.3]	39.8 [45.7]	3.16 Hf [0.97]	Al (10), Cu (20), Fe (10), Mo (20), W (50), Zr (400), C (70), N (30), O (280)
Alloy 55-3H	56.0 [55.4]	34.1 [41.4]	9.61 Hf [3.13]	Zr (1300), Cu (50), Fe (15), Mn (6), Mo (20), Si (80), C (60), N (2), O (180)
Alloy 55-5H	53.5 [55.0]	31.6 [39.9]	14.6 [4.95]	Al (10), Co (20), Cu (90), Fe (10), Mo (20), W (100), C (60), N (<10), O (150)

TABLE 3.—EDS ANALYSIS OF PHASES IN THE ALLOY 55
(SHOWN IN FIGS. 6 AND 7)

Analysis location	Ni, at.%	Ti, at.%	Ni:Ti ratio	Likely compound
A	61.315	38.685	$1.6 \approx 1.5$	Ni_3Ti_2
B	60.428	39.57	1.5	Ni_3Ti_2
C	71.218	28.782	$2.5 \approx 3$	Ni_3Ti
D	72.238	27.762	$2.6 \approx 3$	Ni_3Ti
E	52.012	47.988	$1.1 \approx 1$	NiTi

TABLE 4.—EDS ANALYSIS OF PHASES IN ALLOY 55-1H (FIGS. 8 AND 9)

Analysis location	Ni, at.%	Ti, at.%	Hf, at.%	C, at.%	O, at.%	N, at.%	Ni:Ti ratio	Likely compound
A	61.012	36.762	2.226	0	0	0	$1.6 \approx 1.5$	Ni_3Ti_2
B	53.844	44.106	2.050	0	0	0	$1.2 \approx 1$	Ni(Ti,Hf)
C	4.260	2.575	44.389	10.930	37.846	--------	N/A	HfO_2
D	6.403	61.128	1.450	0	0	31.019	N/A	TiN
E	61.845	36.655	1.50	0	0	0	$1.7 \approx 1.5$	Ni_3Ti_2
F	60.429	37.21	2.357	0	0	0	$1.6 \approx 1.5$	Ni_3Ti_2

TABLE 5.—EDS ANALYSIS OF PHASES IN ALLOY 55-5H (FIGS. 12 AND 13)

Analysis location	Ni, at.%	Ti, at.%	Hf, at.%	C, at.%	O, at.%	N, at.%	Ni:Ti ratio	Likely compound
A	5.457	4.287	51.502	0	38.754	0	N/A	HfO_2
B	45.380	26.591	17.359	10.670	0	0	N/A	HfC[a]
C	50.402	42.119	7.479	0	0	0	1.2	Ni(Ti,Hf)
D	49.721	40.931	9.348	0	0	0	1.2	Ni(Ti,Hf)

[a]Probably includes interference from the Ni(Ti,Hf) parent phase due to the sample volume created by the moderately high excitation voltage.
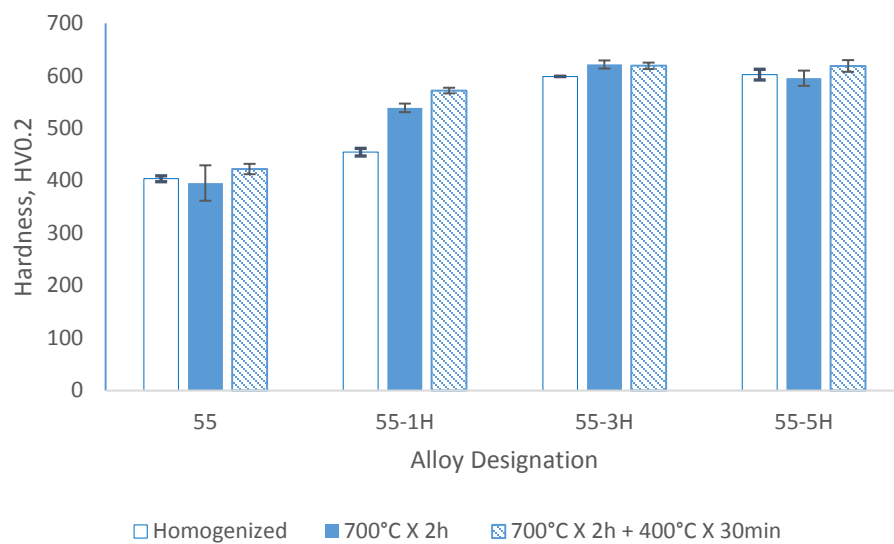
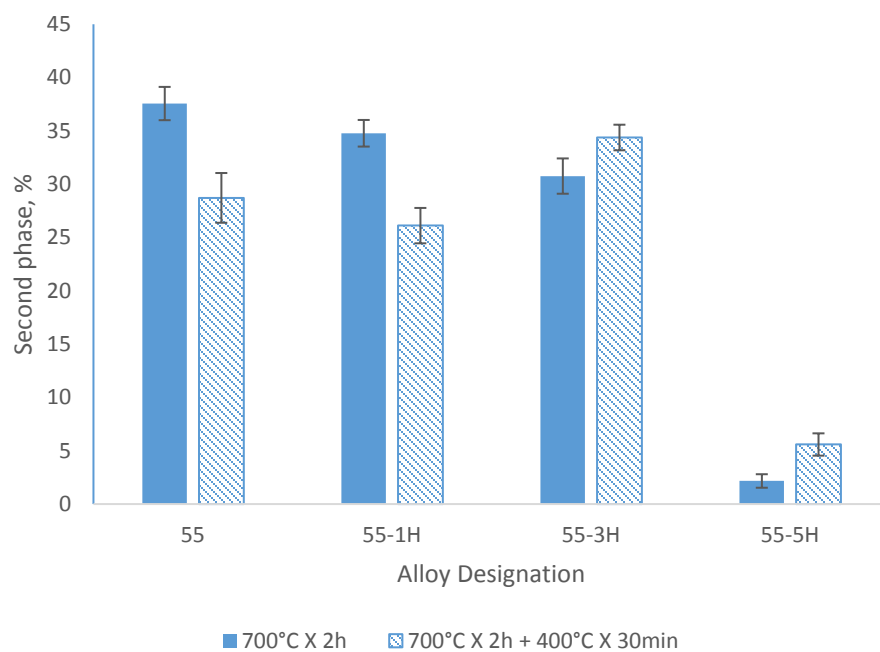Figure 1.—Microindentation hardness of Ni-Ti and Ni-Ti-Hf compounds.

Figure 2.—Volume percent of secondary phases in Ni-Ti and Ni-Ti-Hf compounds.
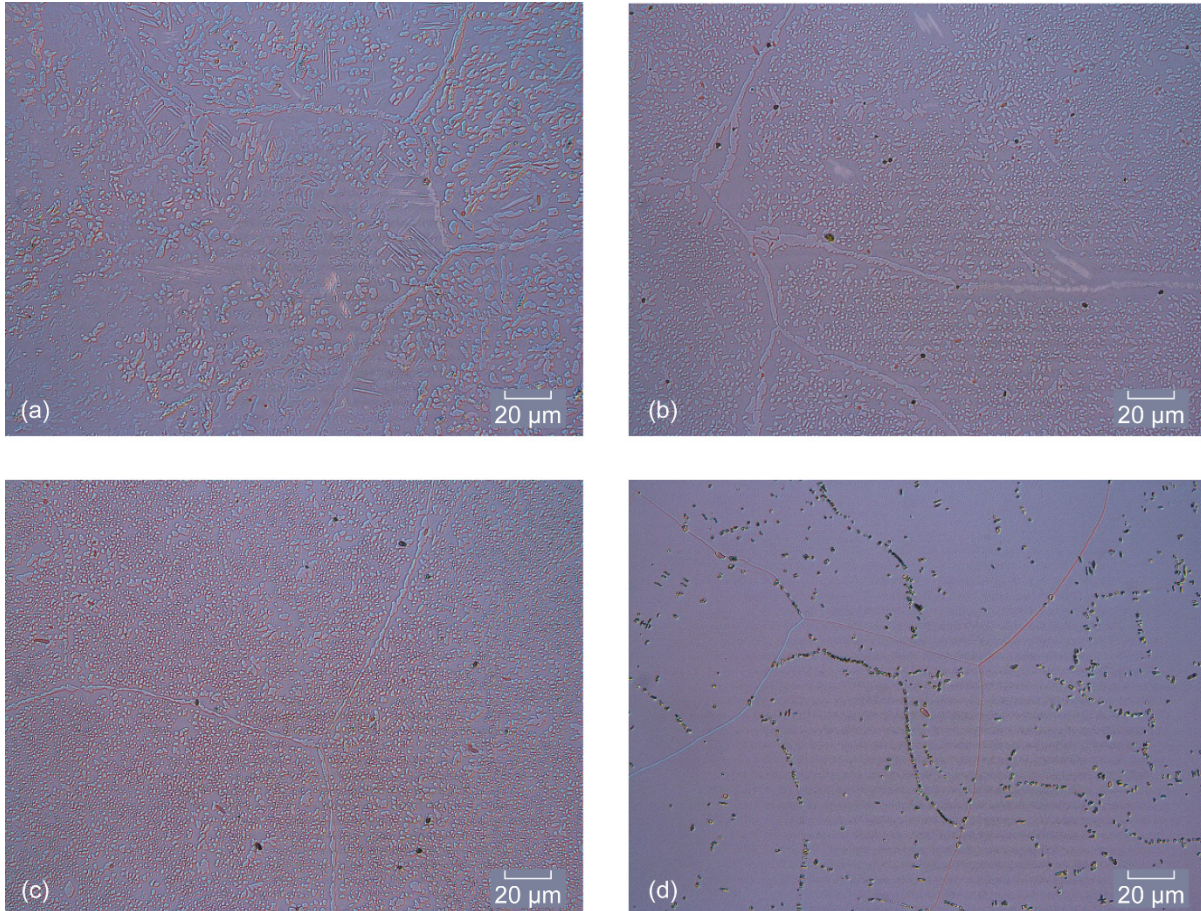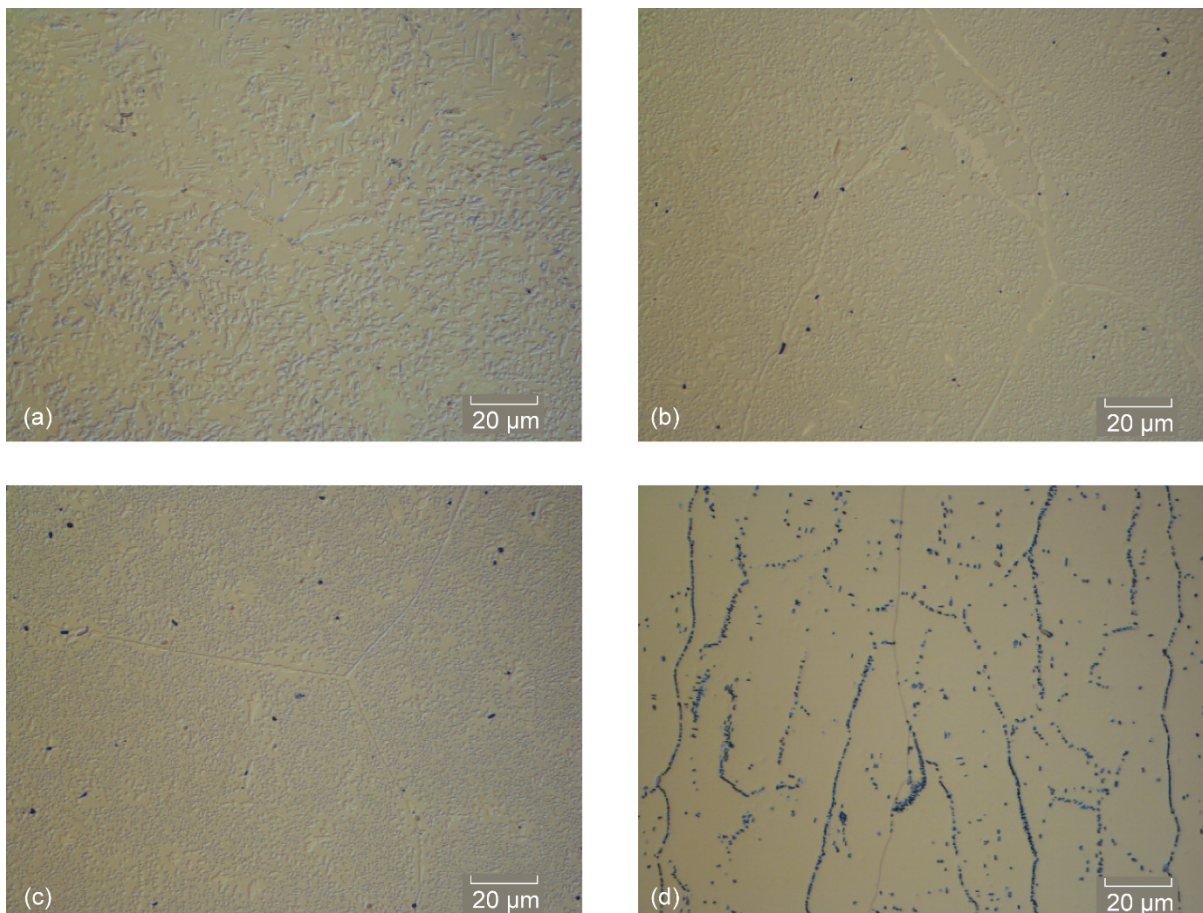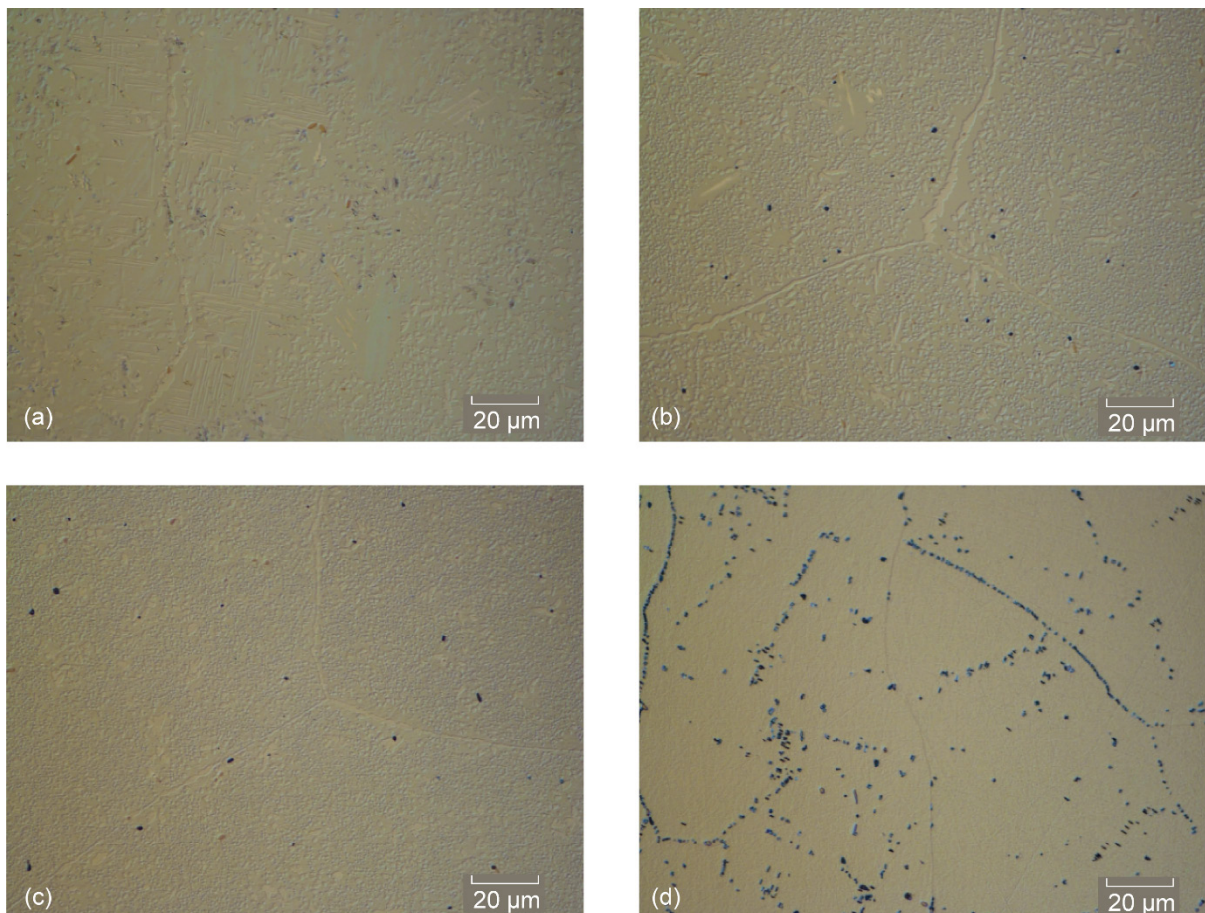
Figure 3.—Optical micrographs of (a) alloy 55 (55 at.% Ni – 45 at.% Ti), (b) alloy 55-1H (55 at.% Ni – 44 at.% Ti – 1 at.% Hf, (c) alloy 55-3H (55 at.% Ni – 42 at.% Ti – 3 at.% Hf and (d) alloy 55-5H (55 at.% Ni – 40 at.% Ti – 5 at.% Hf) after homogenization at 1,050 °C for 48 hr followed by furnace cooling. The specimens are swab-etched using an aqueous solution of 10 vol.% HNO_3 + 1 vol.% HF.

Figure 4.—Optical micrographs of (a) alloy 55 (55 at.% Ni – 45 at.% Ti), (b) alloy 55-1H (55 at.% Ni – 44 at.% Ti – 1 at.% Hf, (c) alloy 55-3H (55 at.% Ni – 42 at.% Ti – 3 at.% Hf and (d) alloy 55-5H (55 at.% Ni – 40 at.% Ti – 5 at.% Hf) after homogenization followed by heat treatment at 700 °C for 2 hr (water quench).

Figure 5.—Optical micrographs of (a) alloy 55 (55 at.% Ni – 45 at.% Ti), (b) alloy 55-1H (55 at.% Ni – 44 at.% Ti – 1 at.% Hf, (c) alloy 55-3H (55 at.% Ni – 42 at.% Ti – 3 at.% Hf and (d) alloy 55-5H (55 at.% Ni – 40 at.% Ti – 5 at.% Hf) after homogenization followed by heat treatment at 700 °C for 2 hr (water quench) and aging at 400 °C for 30 min. (water quench).
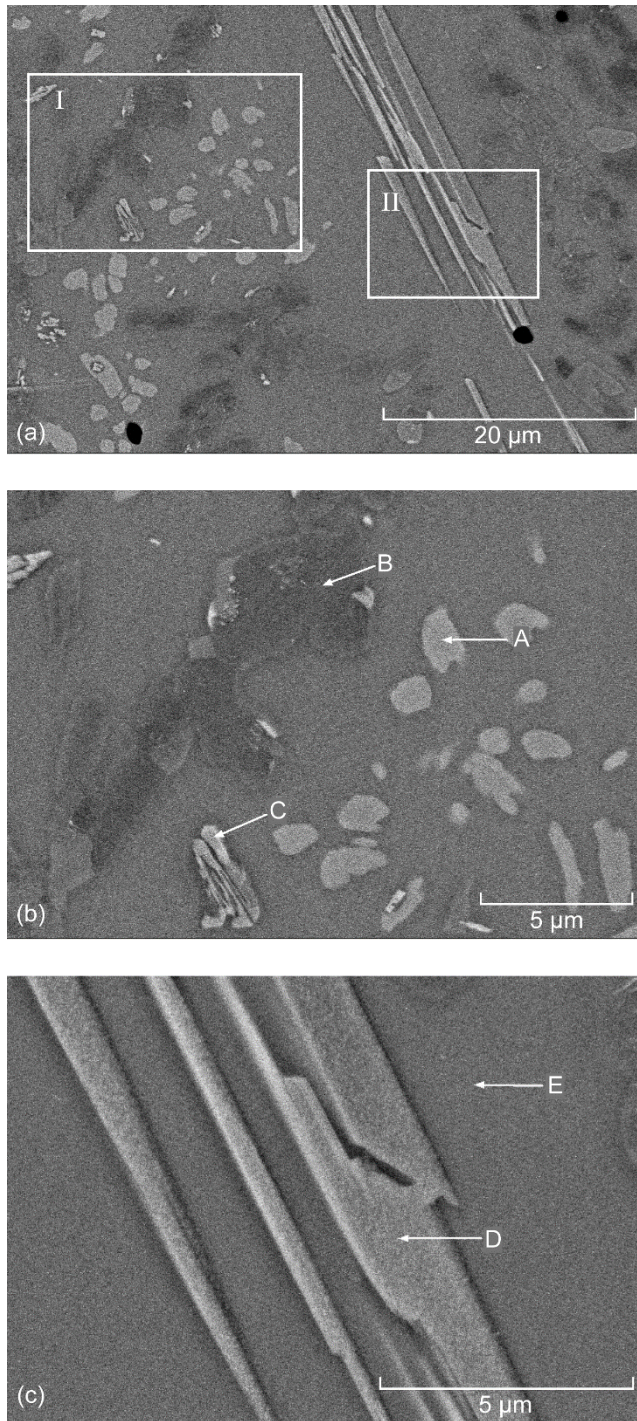
Figure 6.—SEM micrographs of alloy 55 (a) showing second phase precipitates (higher magnification images of (b) region I and (c) region II include labels marking locations of EDS analyses at locations A-E).
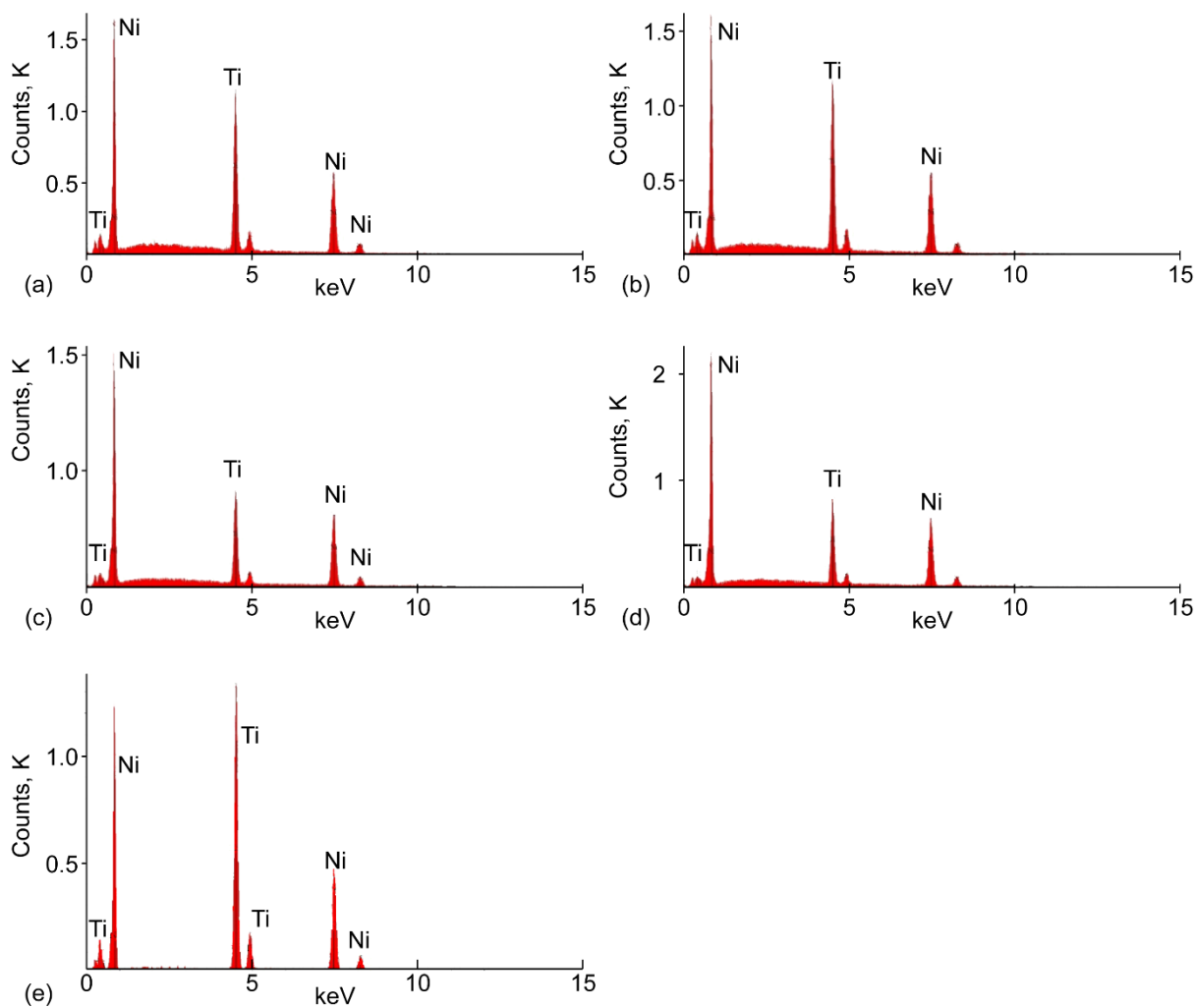
Figure 7.—EDS spectra of phases in alloy 55 (Fig. 6). These data are listed quantitatively in Table 3.
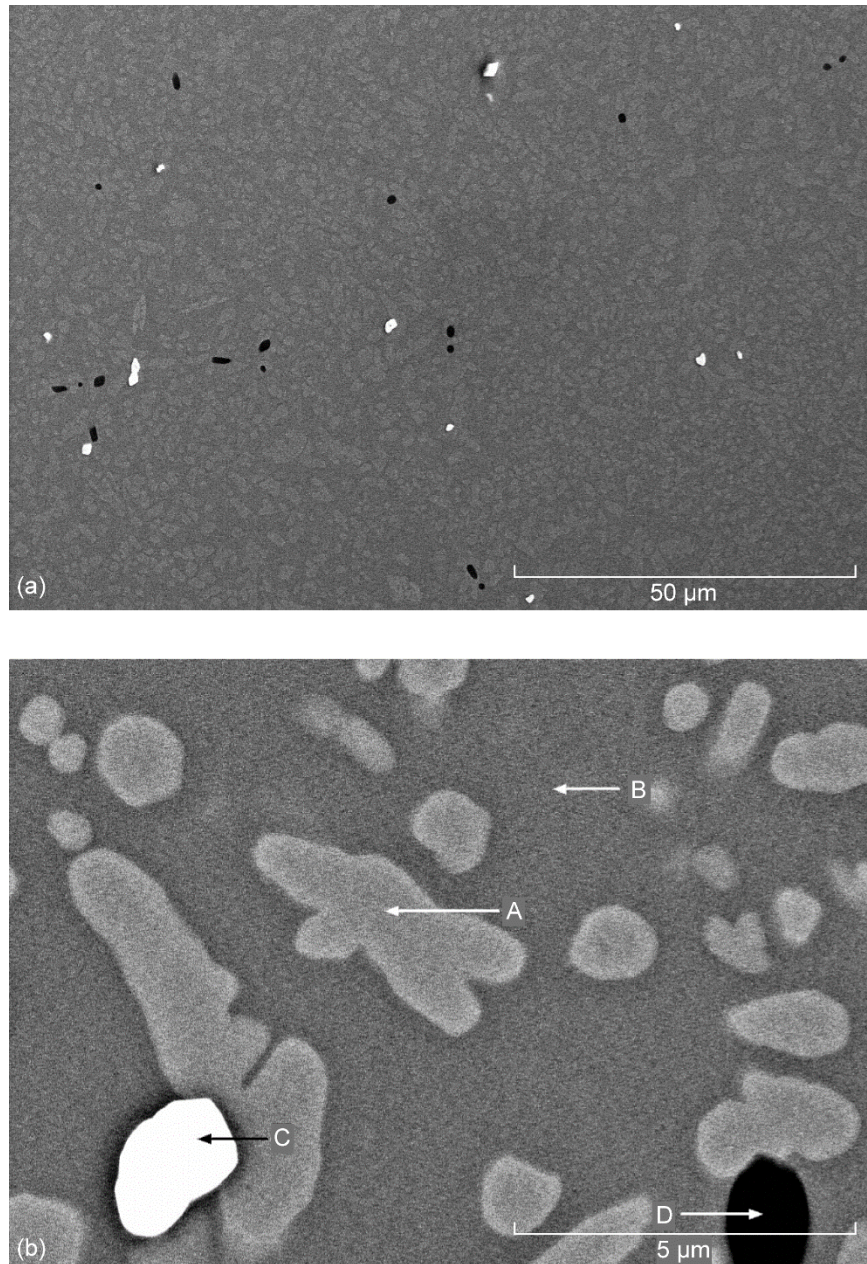
Figure 8.—SEM micrographs at (a) lower and (b) higher magnification of alloy 55-1H showing second phase precipitates within a grain. The labels in Figure 8(b) mark locations of EDS analyses, which indicate the phases are (A) Ni_3Ti_2, (B) Ni(Ti,Hf), (C) HfO_2 and (D) TiN (Fig. 9 and Table 4).
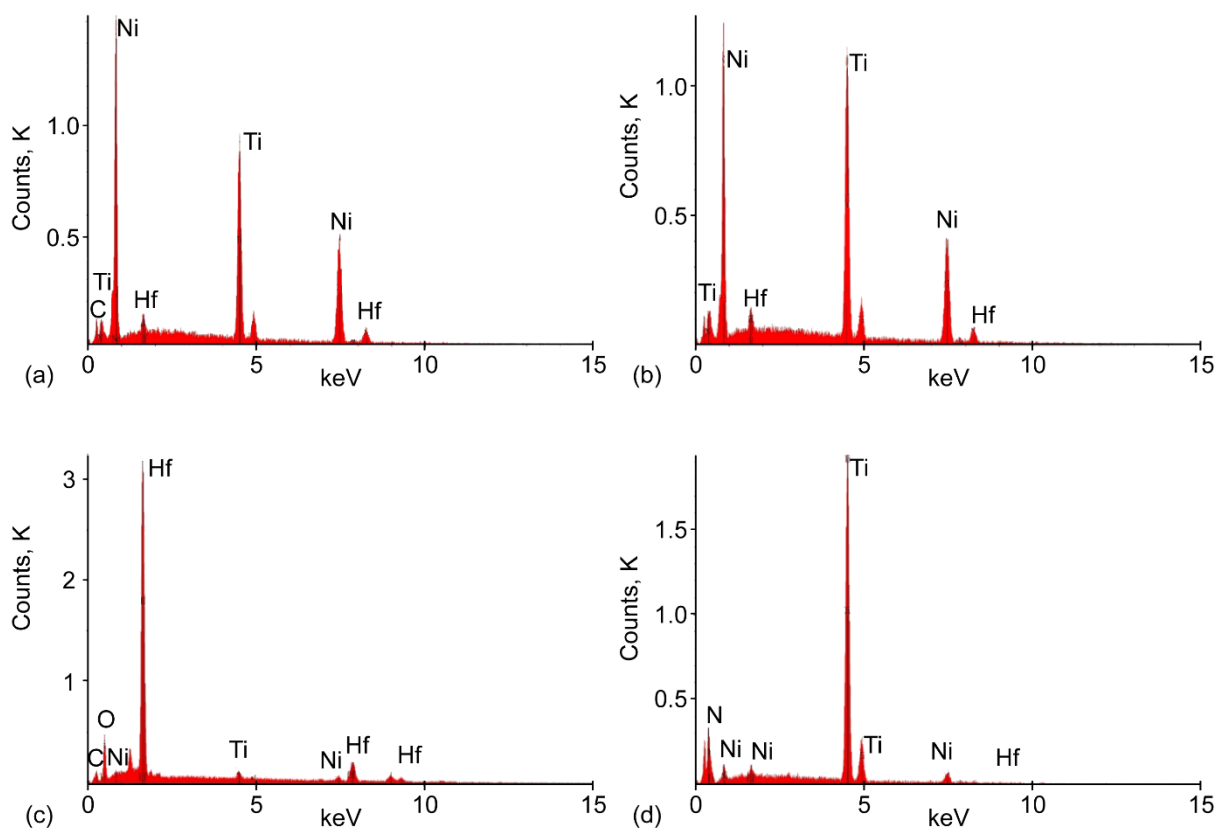
Figure 9.—EDS of second phase precipitates at (a) spot A, (b) spot B, (c) spot C, and (d) spot D (Fig. 8(b)) in alloy 55-1H. Quantitative data from these analyses are listed in Table 4.
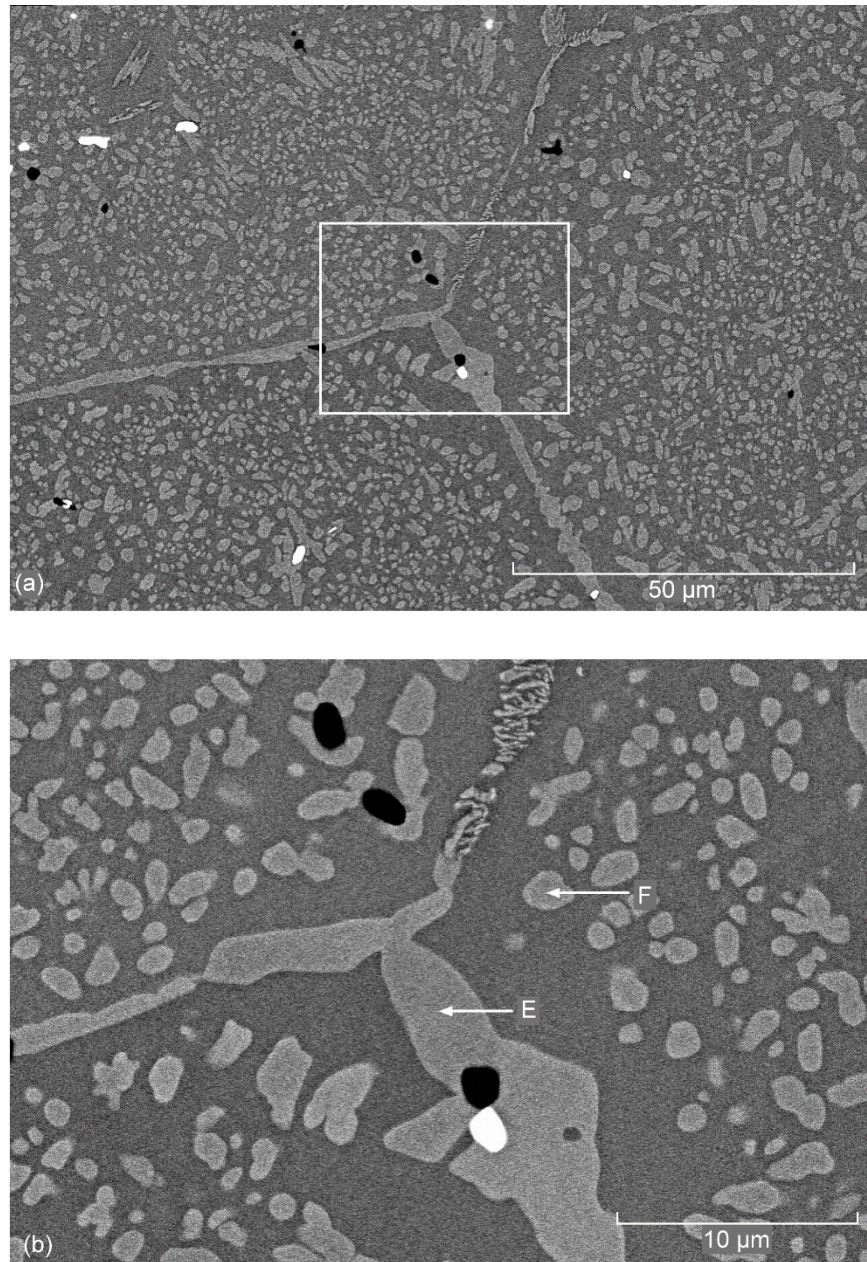
Figure 10.—Additional SEM micrographs of alloy 55-1H at (a) lower and (b) higher magnification showing second phase precipitates along grain boundaries. The labels in Figure 10(b) mark locations of EDS analyses, which indicate the phases are (E) Ni_3Ti_2 and (F) Ni_3Ti_2 (Fig. 11 and Table 4).
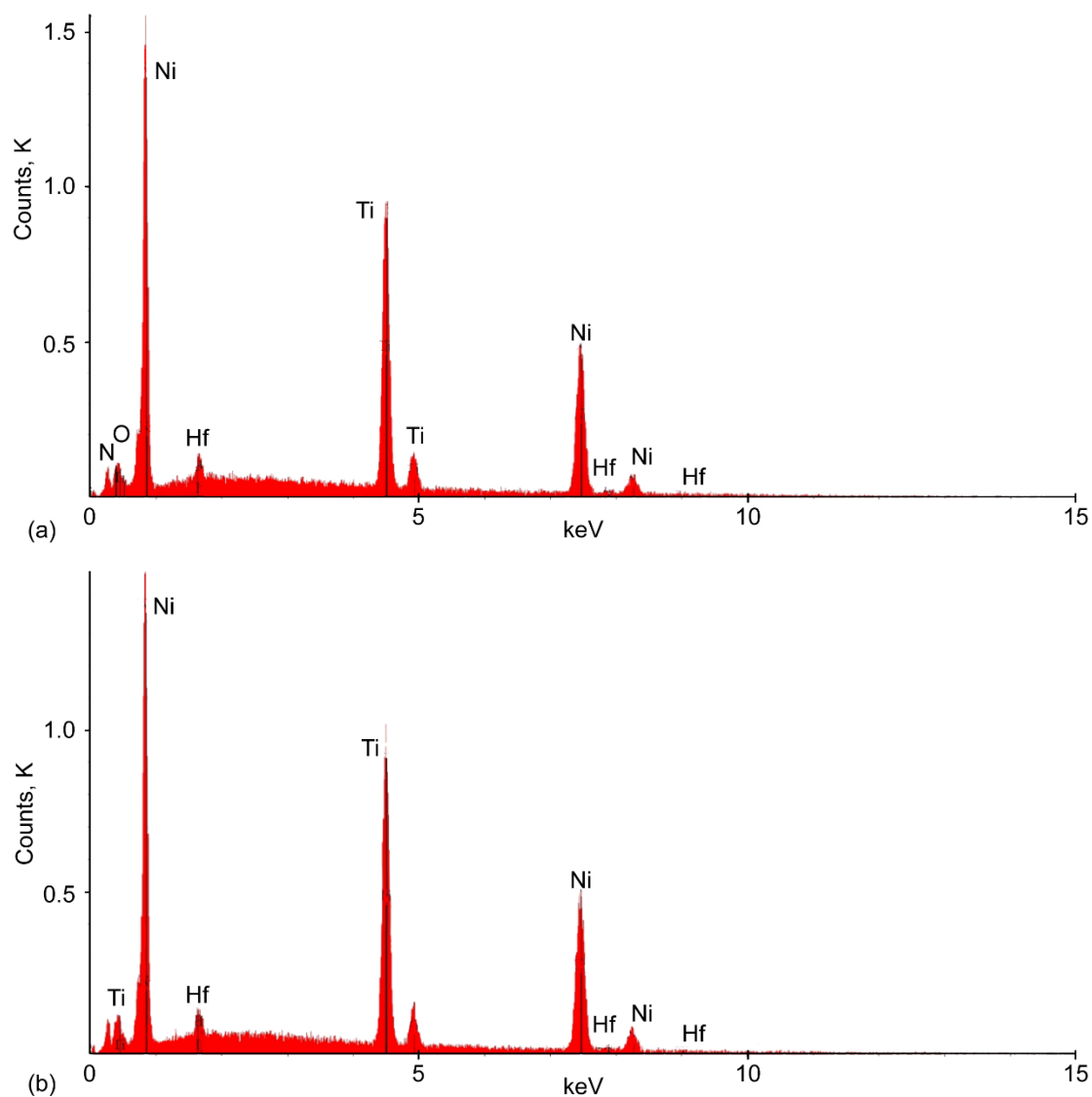
Figure 11.—EDS of second phase precipitates at (a) spot E and (b) spot F (Fig. 10(b)) in alloy 55-1H.
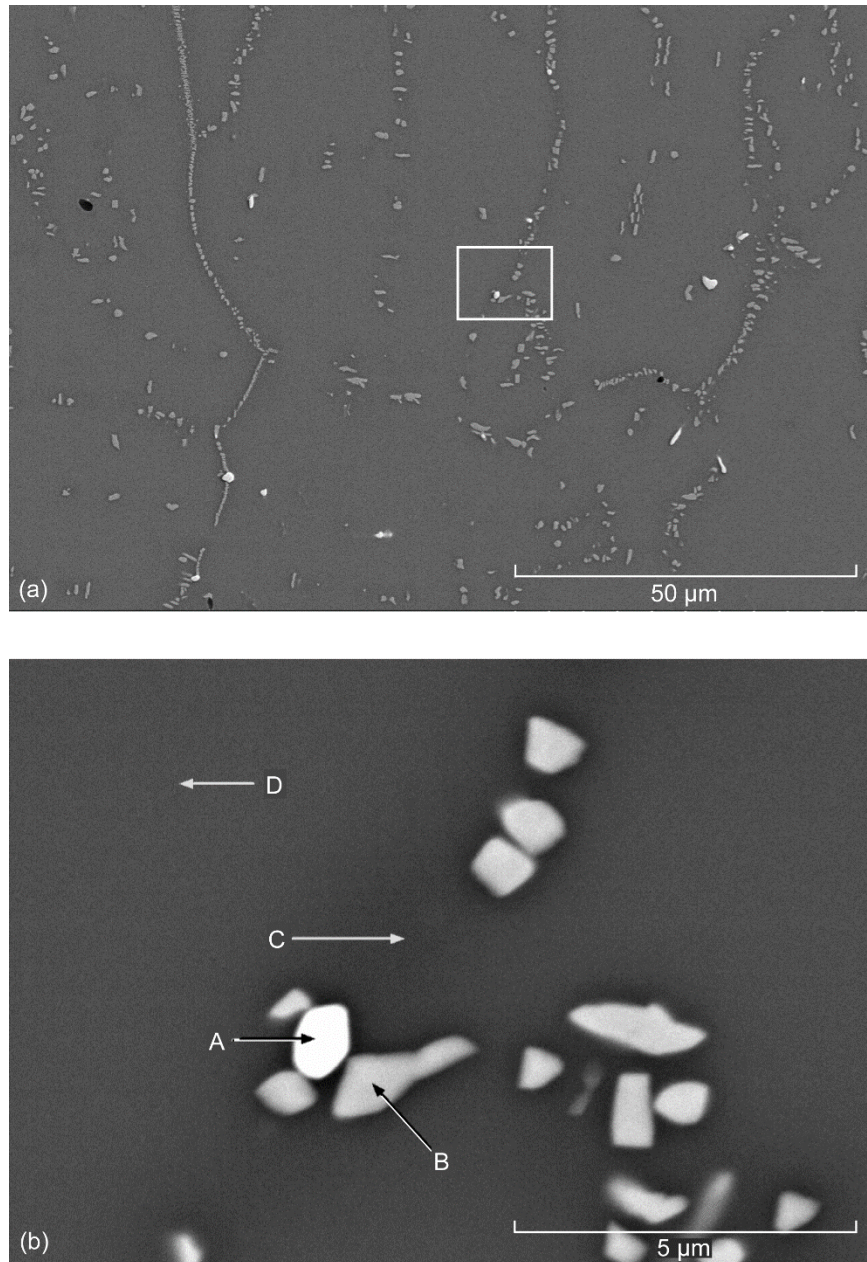
Figure 12.—SEM micrographs of alloy 55-5H at (a) lower and (b) higher magnification showing a few sparse oxide and carbide phases, identified as (A) HfO_2 and (B) HfC in the parent Ni(Ti,Hf) phase (C-D).
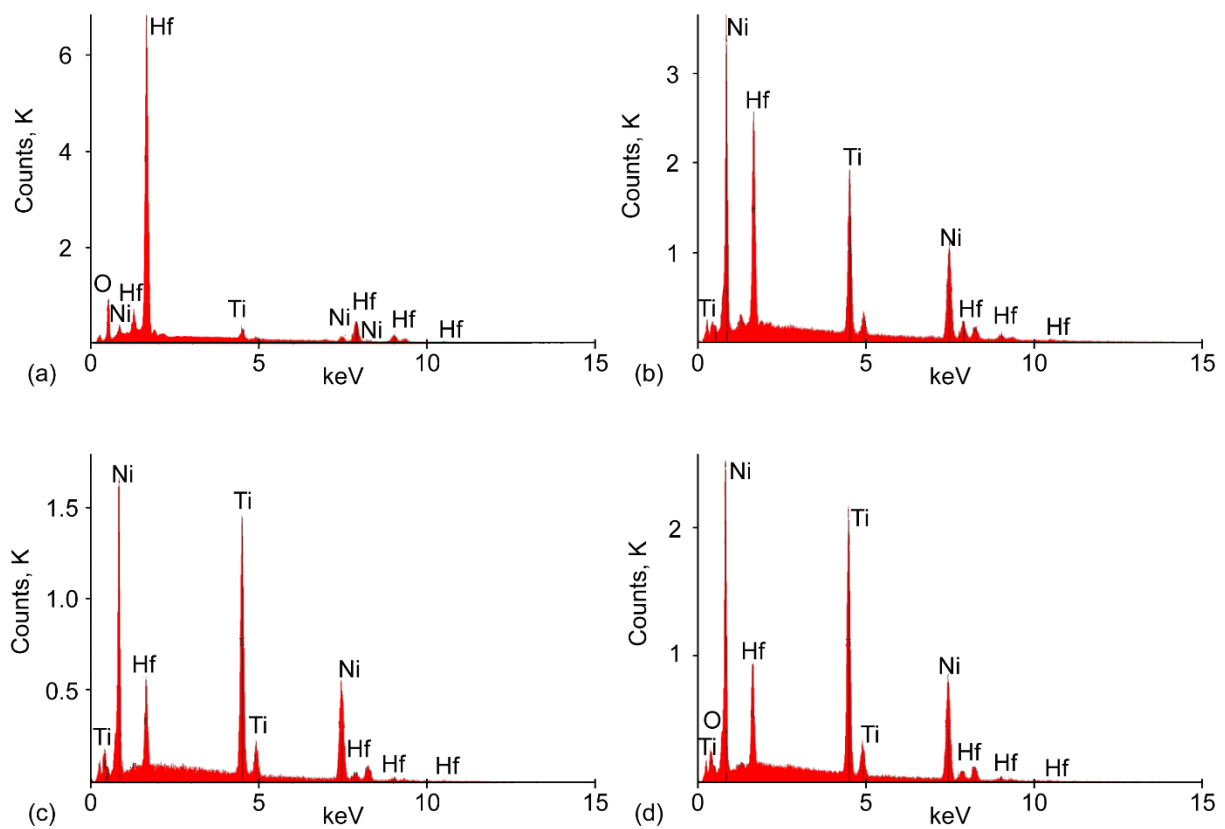
Figure 13.—EDS of alloy 55-5H showing a few sparse oxide and carbide phases in the Ni(Ti,Hf) parent phase.